NUMERICAL MODELLING OF LOW-VELOCITY IMPACT DAMAGE IN FIBRE-METAL-LAMINATES

Jeremy Laliberté and Cheung Poon
IAR-SMPL National Research Council Canada
1200 Montreal Road, Ottawa, ON K1A 0R6, Canada

Paul. V. Straznicky
Department of Mechanical and Aerospace Engineering, Carleton University
1125 Colonel By Drive, Ottawa, ON K1S 5B6, Canada

Keywords*: impact, fibre-metal laminates, finite element modelling, damage*

Abstract

Fibre-metal-laminates (FMLs), a hybrid of metals and fibre-reinforced polymers (FRPs), are a relatively new family of materials available to aircraft designers. Compared to monolithic alloys, these materials combine lower density, higher strength and improved damage tolerance. FMLs must be subjected to the same stringent qualification procedures as any new aircraft material. Susceptibility to impact damage is a property that must be characterized. Traditional composite materials typically develop internal damage when subjected to low-velocity impacts. Determining the response of FMLs under similar loading is an important task to be completed before applying them to impact prone aircraft components.

The objective of this research project was to develop an impact damage modelling methodology for FMLs. A major part of this methodology was the development of a user-defined material subroutine in LS-DYNA for the FRP in one type of FML. The results of the modelling showed that delamination is not a critical damage mode in FMLs under low-velocity impact loads.

1 Introduction

This paper describes the results of a series of low-velocity impact experiments and simulations conducted on GLARE (GLAss REinforced) laminates.

The experimental portions of this work were conducted as part of the FML Durability Project. This project is a multi-year collaborative effort between the Structures, Materials and Propulsion Laboratory of the Institute for Aerospace Research (IAR-SMPL), Bombardier Aerospace and Carleton University to investigate the behaviour of GLARE under various loading conditions. The impact tests and post-impact inspections were carried out at IAR-SMPL. The modelling was performed at the Department of Mechanical and Aerospace Engineering of Carleton University.

1.1 Fibre-Metal-Laminate Technology

Early research demonstrated that laminating thin sheets to form thick plates increased the fracture toughness of aluminum. The fracture toughness of the laminated plates approaches that of the thin constituent sheets [1]. Researchers at the Technical University of Delft (TUDelft) in the 1970s improved upon this by adding aramid fibres to the laminates to further enhance the fatigue crack growth resistance [2]. The resulting FMLs are composed of layers of metal and FRP bonded together. The laminate possesses increased strength, reduced density and improved damage tolerance over monolithic alloys and conventional composites [3,4].

These materials are being applied on the Airbus A380 airliner as a primary fuselage material. GLARE and ARALL (Aramid
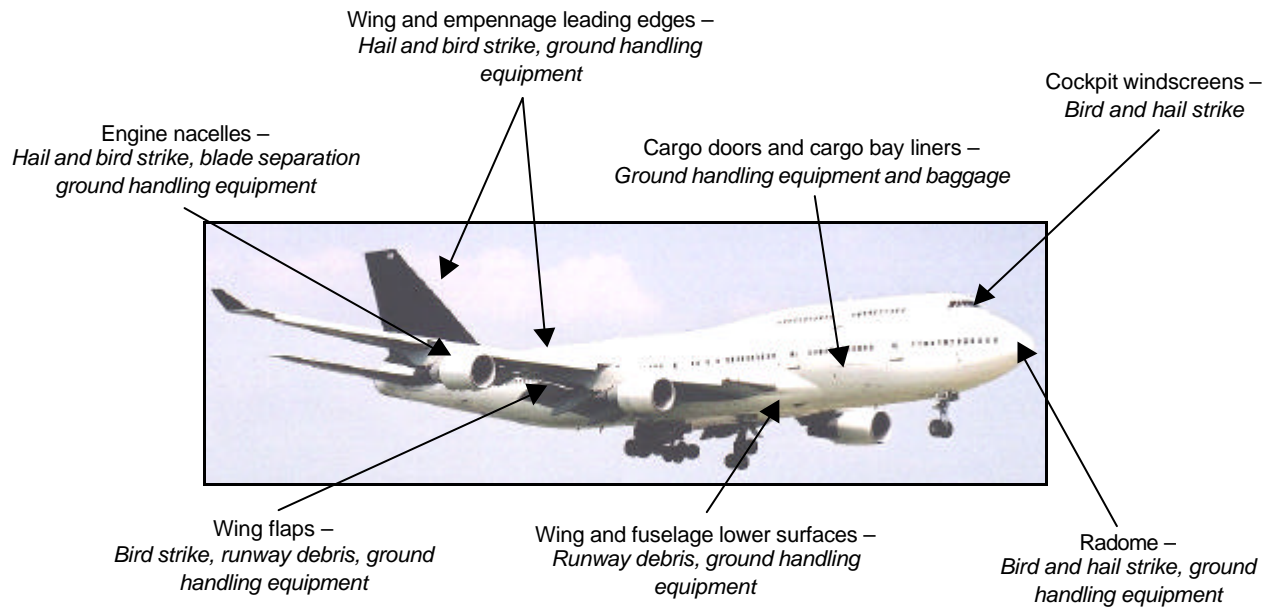
Fig. 1. Impact prone areas on a modern transport aircraft.

Reinforced Aluminum Laminates) are already used in impact prone cargo bay floors and wing flaps. Exposure of these materials to impact will increase as they are applied in more locations on airframes. Fig 1. summarizes impact prone areas and highlights the sources of impact damage.

A major component of the FML Durability Project has been the investigation of the impact damage tolerance of GLARE laminates beginning with an extensive review of the state-of-the-art. An in-depth testing program and simulations of the response of impacted GLARE panels followed [5,6,7]. Additionally, post-impact damage tolerance under fatigue, tensile and shear loading was evaluated [8,9,10].

1.2 Review of Testing and Modelling of Low-Velocity Impacts on FMLs

Numerous researchers have reported results of low-velocity impact tests on FMLs as summarized in Table 1. This table also lists the types and configurations of the tests. Also listed is the size of the test specimen and size of the test area. A detailed summary of these methods is provided in [5]. The abbreviations in the table are CARALL (CArbon Reinforced ALuminum Laminate), CFRP (Carbon Fibre Reinforced Polymer), GFRP (Glass fibre

reinforced Polymer) and AFRP (Aramid Fibre Reinforced Polymer).

In general, these results showed that GLARE will out-perform aluminum under impact loading in terms of absorbed energy [11,12]. GLARE will also develop a visible dent, similar to monolithic alloys, when subjected to impact. This dent provides clear visual evidence that an impact has taken place. Traditional composites will develop significant internal damage with little surface indications when subjected to the same impact energy levels [11,13].

Impact tests are typically time consuming and because of scatter in the results, require large sample sizes. Therefore some efforts have been undertaken to model the response of FMLs. Table 2 summarizes some of the recent analytical and finite element models have been developed for FMLs. Delamination was only incorporated into the FEA models to model damage from in-plane and out-of-plane peel loads. Some analytical techniques have been developed for impact loading [11,14]. However, these models do not account for stiffness loss in the FRP layers as micro-cracks develop; nor do they account for delamination damage. These analytical models are further limited since they are developed for specific geometries and cannot be applied to complex

TABLE 1. Summary of impact test methods.

Reference	Materials Tested	Test Type	$r_{impactor}$ (mm)	Coupon Size (mm)	Test Area (mm)
[4]	CARALL	Drop and gas gun	6.35	101.6 x 101.6	Not available
[11]	2024-T3, CFRP, AFRP, GLARE, ARALL	Drop	7.5	100 x 100	ϕ 80
[11]	2024-T3, CFRP, GFRP, AFRP, ARALL	Drop	7.5	150 x 150	100 x 100
[11]	CFRP, GLARE, ARALL, CARALL	Drop	5 and 7.5	100 x 100	ϕ 80
[16]	CFRP, ARALL	Drop	12.7	76 x 406	ϕ 50.8
[17]	ARALL	Pendulum	6.35	127 x 254	Not available
[14]	ARALL	Gas gun	6.35	101.6 x 25.4	Not available
[18]	CFRP, GFRP, AFRP, GLARE, various aluminum honeycomb combinations	Drop and bird strike	8.0	100 x 150	75 x 125
[12]	2024-T3, CFRP, GFRP, AFRP, ARALL	Drop	7.5	100 x 100	ϕ 80
[19]	2024, 7075, GLARE	Drop	8	100 x 100	ϕ 76

TABLE 2. Summary of FML modelling techniques.

Reference	Application	Type	Capabilities	Limitations
[20]	Static loading simulations	FEA	Damage in the prepreg,	No delamination
[21]	Static loading simulations	FEA	Elastic-plastic behaviour of aluminum	No delamination
[22]	Delamination fatigue	FEA	Delamination included	No plasticity, prepreg elastic up until failure,
[12]	Impact	Non-linear Analytical	Elastic plastic behaviour of aluminum	No delamination, assumed elastic prepreg
[11]	Impact	Linear Analytical	Can model contact forces	No delamination, assumed elastic prepreg
[14]	Impact	Non-linear Analytical	Can model contact forces, can model dent depth	No delamination, assumed elastic prepreg

parts. Finite element methods would make the simulation of complex parts possible. However, current FEA models are limited to static rather than impact loading.

It was therefore decided to develop a new test program to examine several GLARE variants subjected to low-velocity impact loads. This testing was coupled with a series of finite element simulations to develop a methodology for reducing the amount of testing required for future types of FMLs.

2 Impact Testing at IAR-SMPL

Based on this review of the state-of-the-art in FML impact testing it was decided to conduct additional impact tests on more recently developed materials.

There is no standard test method for low-velocity impact on FMLs. Therefore, the NASA standard impact test method [15] for composites was initially used. This test fixture, which clamps the specimen over a square opening of 127 mm x 127 mm, introduced undesirable deformation at the corners of the
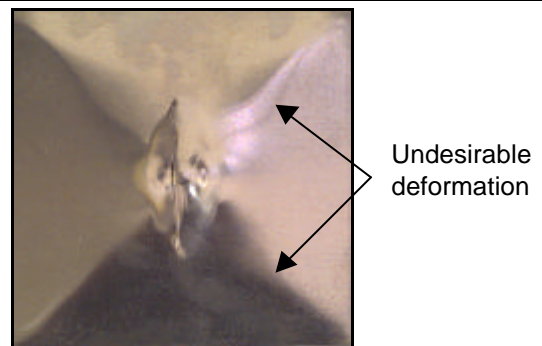

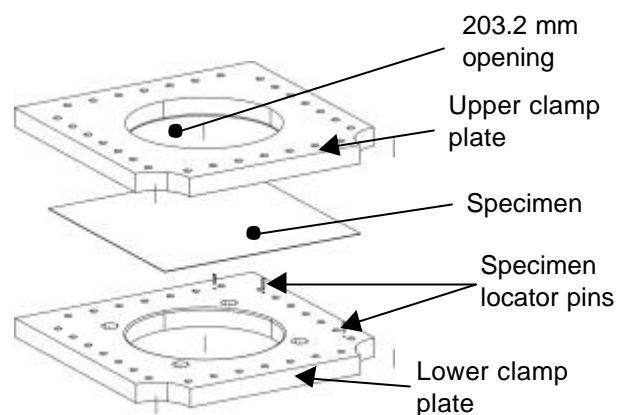Fig 2. Typical deformation from the NASA fixture.
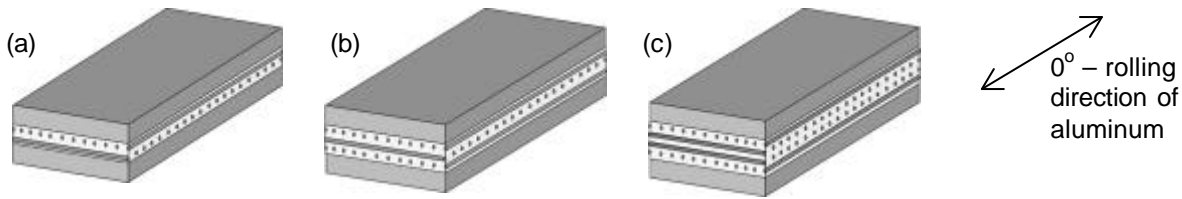

Fig. 3. IAR-SMPL FML impact fixture.

Fig. 4. (a) GLARE-3-2/1, (b) GLARE-4-2/1 and GLARE-5-2/1 variants used in the low-velocity impact tests.

impacted area as shown in Fig. 2. To reduce the edge deformation, a new impact fixture was designed following these tests specifically for FMLs (Fig. 3).

2.1 Impact Test Procedure

Three types of GLARE, as shown in Fig. 4, were tested according to the test matrix in Table 3. The impact fixture was installed into the Dynatup drop weight impact tower located at IAR-SMPL (Fig. 5). The panels were subjected to impact energies ranging from 15 J to 65 J with a 6.75 kg mass and a 25.4 mm diameter steel impactor. Impact force data was collected with an instrumented load cell. The velocity just before impact was measured with an infrared timing gate and combined with the force data to calculate impact energy and displacement. Impacted panels were inspected using a penetrant-enhanced x-ray technique and destructive cross-sectioning.

TABLE 3. Impact test matrix.

Material	Impact Energy Level							Total
	15	25	35	45	55	60	65	
2024-T3	0	6	6	6	6	6	0	32
GLARE-3	6	6	6	6	6	0	0	32
GLARE-4	0	6	6	6	6	6	0	32
GLARE-5	0	6	6	6	6	0	6	32
Total	6	24	24	24	24	12	6	128

2.2 Experimental Results

Detailed descriptions of the results of the low-velocity impact tests conducted on GLARE have been published elsewhere [5,6,7]. Three parameters of particular interest in this study were the energy absorbed (E_{abs}), peak impact force (F_{max}) and the permanent dent depth (d_{perm}). The absorbed energy can be used as a measure of total damage suffered by the coupon; however, this value also includes stored elastic energy and system losses. The
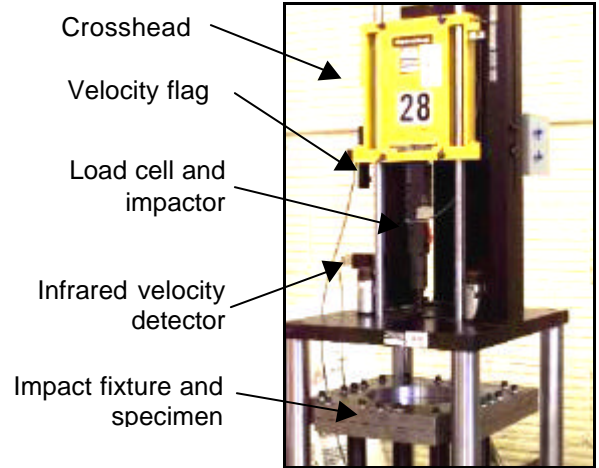

Fig. 5. IAR-SMPL Dynatup drop weight impact tower.

peak impact force is a measure of the overall stiffness of the coupon being impacted. The measured values will be compared to simulation results in subsequent sections.

3 Damage Modelling Methodology

The explicit finite element code LS-DYNA from LSTC was used for the impact simulations [23]. This code is well-suited to dynamic problems with large deformations and has been employed at Carleton University for simulating impact on conventional composites [24]. An important feature of this code is the ability to simulate delamination using the tiebreak-interface. The user can specify "normal" and "shear" strengths for the interface based on material properties. The interface ties two surfaces together until failure is reached; the surfaces are then released. If no failure is modelled then the surfaces are connected using a tied-interface. A tied-interface connects all degrees of freedom between the two layers.

Initial simulations of monolithic aluminum panels resulted in the selection of thick-shell elements for the GLARE panels. Thick-shells are a hybrid of solid brick and

thin-shell elements and do not suffer the aspect ratio problems to which solid-bricks are prone.

The damage modelling methodology requires four components to accurately predict the response of GLARE panels as listed below. Each of these components was evaluated separately.

1. Material model for the aluminum
2. Delamination initiation criterion
3. Delamination growth model
4. Material model for the FRP

An accurate material model for the aluminum must include plasticity effects for modelling the post-yield behaviour of the laminate. The delamination initiation criterion and the growth model are inherently linked to one another. Experimental evidence showed that delamination occurred in these laminates at relatively low energy levels. It was not possible to determine from the experiments if the contribution of delamination to the overall impact response was significant. Therefore, the simulations were intended to provide this information. To provide interfacial property data on GLARE, a series of double-cantilever beam tests were carried out [25]. After the tests were completed it was determined that it was not possible to use this information in LS-DYNA due to the complex stress-state at the crack tip. Therefore, the quoted manufacturer's properties for the interface were employed with the tiebreak-interface.

3.1 Development of a User-Defined Material Subroutine in LS-DYNA

A user-defined material subroutine (UMAT) was developed based on continuum-damage mechanics (CDM) theories. Continuum damage mechanics can be used to describe the cumulative effect of the deterioration of a material through the formation of microcracks by using a field variable, d, to denote the level of damage or deterioration [26]. The damage strain energy release rate is a function of the change in strain energy as shown in (1) [27, 28].

$$Y = \frac{1}{2}\frac{dE_e}{dd} \qquad (1)$$

This relationship (1) for the damage variable provides a link between the strain energy and damage and has been used to describe the formation of damage in an individual ply [29]. A version of this model was also implemented as a stand-alone FEA code to model static tensile tests on GLARE-2 [30]. Ladevèze and Le Dantec (1992) developed the relationship in (2) for the damaged material strain energy, E_D.

$$E_D = \frac{1}{2}\left[\begin{array}{c} \dfrac{\boldsymbol{s}_{11}^2}{E_{11}^0} - 2\dfrac{\boldsymbol{n}_{12}^0}{E_{11}^0}\boldsymbol{s}_1\boldsymbol{s}_2 + \dfrac{\langle\boldsymbol{s}_{22}\rangle_+^2}{E_{22}^0(1-d')} + \dfrac{\langle\boldsymbol{s}_{22}\rangle_-^2}{E_{22}^0} \\ + \dfrac{\boldsymbol{s}_{12}^2}{G_{12}^0(1-d)} + \dfrac{\boldsymbol{s}_{13}^2}{G_{12}^0(1-d)} + \dfrac{\boldsymbol{s}_{23}^2}{G_{23}^0} \end{array} \right] \quad (2)$$

where the subscripts 1, 2 and 3 denote the fibre direction, the transverse direction and the through-thickness direction, respectively. The angled brackets and the $\pm$ subscripts indicate negative or positive conditions for $\boldsymbol{s}_{11}$; therefore, if $\boldsymbol{s}_{22}$ is positive then $\langle\boldsymbol{s}_{22}\rangle_-^2$ is equal to zero. This allows different compressive and tensile conditions to be modelled. E_{11} is the modulus in the fibre direction and E_{22} is the modulus in the transverse direction. The damage variable (d') associated with E_{22} allows the difference in tensile and compressive behaviour to be modelled. When $\boldsymbol{s}_{22}$ is compressive (negative) the matrix cracks close and do not affect the modulus. The two damage variables (d and d') act upon the initial transverse modulus and the shear modulus, (E_{22}^0 and G_{12}^0) as shown in (3).

$$G_{12} = G_{12}^0(1-d)$$
and $\qquad (3)$
$$E_{22} = E_{22}^0(1-d')$$

Furthermore, two dissipation variables are associated with the damage terms d and d':

$$Y_{d'} = \boldsymbol{r}\frac{\partial \boldsymbol{y}}{\partial d}\bigg|_{\bar{\boldsymbol{s}},d'} = \frac{\partial E_D}{\partial d}\bigg|_{\bar{\boldsymbol{s}},d'} = \frac{1}{2}\frac{\boldsymbol{s}_{12}^2}{G_{12}^0(1-d')^2}$$

$$Y_d = \boldsymbol{r}\frac{\partial \boldsymbol{y}}{\partial d}\bigg|_{\bar{\boldsymbol{s}},d} = \frac{\partial E_D}{\partial d}\bigg|_{\bar{\boldsymbol{s}},d} = \frac{1}{2}\frac{\langle\boldsymbol{s}_{22}\rangle_+^2}{E_{22}^0(1-d)^2} \qquad (4)$$

where $\boldsymbol{y}$ is the free energy density.

Two mechanisms were identified that contribute to the development of damage: matrix micro-cracking and fibre/matrix de-bonding. The following two quantities were introduced to describe the development of the damage [29]:

$$\underline{Y} = (\sqrt{Y_d + bY_{d'}})$$
$$\underline{Y}' = (\sqrt{Y_{d'}}) \tag{5}$$

The damage development laws follow in (6 and 7) [29]:

$$d = \frac{\langle \underline{Y} - Y_0 \rangle_+}{Y_c} \tag{6}$$

if $d<1$ and $\underline{Y}' < Y_s'$; otherwise $d=1$ and the element fails. As well:

$$d' = \frac{\langle \underline{Y} - Y_0' \rangle_+}{Y_C'} \tag{7}$$

if $d'<1$ and $\underline{Y}'<Y_s'$; otherwise $d'=1$ and the element fails. The parameters Y_c, Y_c', Y_0, Y_0' and b are characteristics of the material and are determined by tension tests as well as a few loading-unloading cycles on basic glass-reinforced laminae [29]. The value Y_s' is the brittle-damage threshold that determines the behaviour of the fibre-matrix interface in the element transverse direction

The above model was adapted as a user-defined material subroutine within LS-DYNA for the present work using the following steps. It is evident from (6 and 7) that:

$$\underline{Y} = dY_c + Y_o = d'Y_c' + Y_o' \tag{8}$$

It is then possible to isolate d':

$$d' = \frac{dY_c + Y_o - Y_o'}{Y_c'} \tag{9}$$

Substituting (3, 5 and 9) into (7) gives:

$$(dY_c - Y_o)^2 -$$
$$\frac{1}{2}\frac{s_{12}^2 + s_{13}^2}{G_{12}(1-d)^2} + \frac{b}{2}\frac{s_{22}^2}{\left(1 - \dfrac{dY_c + Y_c - Y_o'}{Y_c'}\right)^2} = 0 \tag{10}$$

TABLE 4. Summary of GLARE-3-2/1 input parameters.

Property	Units	Value
Y_o	MPa$^{1/2}$	0.12
Y_o'	MPa$^{1/2}$	0.00
Y_c	MPa$^{1/2}$	2.00
Y_c'	MPa$^{1/2}$	2.30
b	none	3.40
Y_s	MPa$^{1/2}$	1.10
Y_r	MPa$^{1/2}$	2.00
E_{11}	GPa	53.98
E_{22}	GPa	9.412
E_{33}	GPa	9.412
G_{12}	GPa	3.310
n_{12}	none	0.330
n_{13}	none	0.058
n_{23}	none	0.058

A check for $\underline{Y} - Y_o > 0$ must be performed; if this condition is not met then $d = d' = 0$. Equation (10) has 6 roots and must be solved numerically. The only valid value of d is slightly negative when the stresses are zero. As the applied stress increases, the value of this root increases. None of the other possible solutions exhibit the same behaviour and none of them increase with increasing applied load between 0 and 1. Since the range of valid values for d is known to be between 0 and 1, it is best to use the Bisection Method to find the root. When the stress reachs the rupture limit of the material the root becomes complex. At this point, it is not possible to find a root in the required range, therefore, the critical damage level has been reached and the element fails.

As shown in (3), the damage parameters modify the moduli of the material. In LS-DYNA the damage variables (d and d') are incorporated directly into the constitutive equation for the orthotropic material to decrease the stiffness of the FRP as damage develops. When the damage reaches the critical level defined by [29] the tensile stress in the element is reduced to zero. The element is still permitted to carry compressive stresses, as would occur in an actual impacted panel.

4 Simulation of Impacts on GLARE

The components of the methodology described in the previous section were assembled and used to model the impact response of GLARE-3-2/1, GLARE-4-2/1 and GLARE-5-2/1. In the interest of brevity, this paper will focus on simulation results from GLARE-3-2/1.

4.1 Input Parameters

The input parameters were varied to determine their effect on predicted response. Energy levels for impact were chosen for comparison with the experimental results. The following simulation configurations were developed:
1. Elastic-plastic aluminum, elastic prepreg and tied-interface,
2. Elastic-plastic aluminum, elastic prepreg and tiebreak-interface,
3. Elastic-plastic aluminum, damageable prepreg (UMAT) and tiebreak-interface.

The mesh geometry for the simulations is shown in Fig 6. The impactor and test area had the same dimensions as the IAR-SMPL impact test fixture. The specimen edges were fully clamped. An initial velocity was applied to the impactor to give the appropriate impact energy. The input parameters for the model are summarized in Table 4.
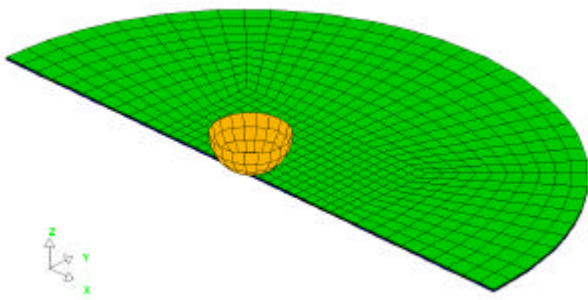

Fig. 6. Mesh geometry for LS-DYNA simulations.

4.2 Simulation Results

Sample predicted delamination damage maps are shown in Figs. 7. These images show that by using the UMAT with a tiebreak-interface it is possible to improve the predicted damage geometry in the GLARE. The percent difference between the measured and predicted absorbed energy, peak impact force and permanent dent depth are shown in Figs. 8-10.

The tied-interface fixed the layers together without failure. These simulations, with elastic prepreg, under-predicted the absorbed energy. The predicted permanent dent depths from these simulations were less than the experimental values. The peak impact force was over-predicted. Both the plasticity of the aluminum and damage in the prepreg contributed to the permanent deformation of the experimentally impacted panels. Without the inclusion of damage in the prepreg layers, energy can only be absorbed through aluminum plastic deformation and stored elastic energy in the prepreg layers. As well, with only the aluminum plasticity contributing to the permanent deformation, the dent depths would be lower. In fact, the elastic stresses in the prepreg layers actually try to push the aluminum layers upward but were prevented from doing so by the lack of delamination. Without the formation of damage, the effective stiffness of the simulated panels with the tied-interface is higher than the actual panels, resulting in the higher impact force predictions.

The simple-tiebreak interface used the FML manufacturer's interface properties to predict failure. Simulations using this interface model, with the elastic prepreg, under-predicted the absorbed energy by the largest amount. The simple-tiebreak interface also resulted in lower dent depths than measured in the experiments. Finally, these simulations over-predicted the peak impact force. The formation of delamination damage was enabled in these simulations, permitting the rebound of the elastic prepreg layers. This released stored elastic energy in the prepreg layers, resulting in the lower absorbed energy prediction. The same action also pushed the aluminum layers upward, leading to considerably lower dent depths than the tied-interface simulations. The peak impact force difference was slightly higher than that of the tied-interface simulations. The small difference indicates that the formation of delamination damage does not have a large influence on the predicted impact force.
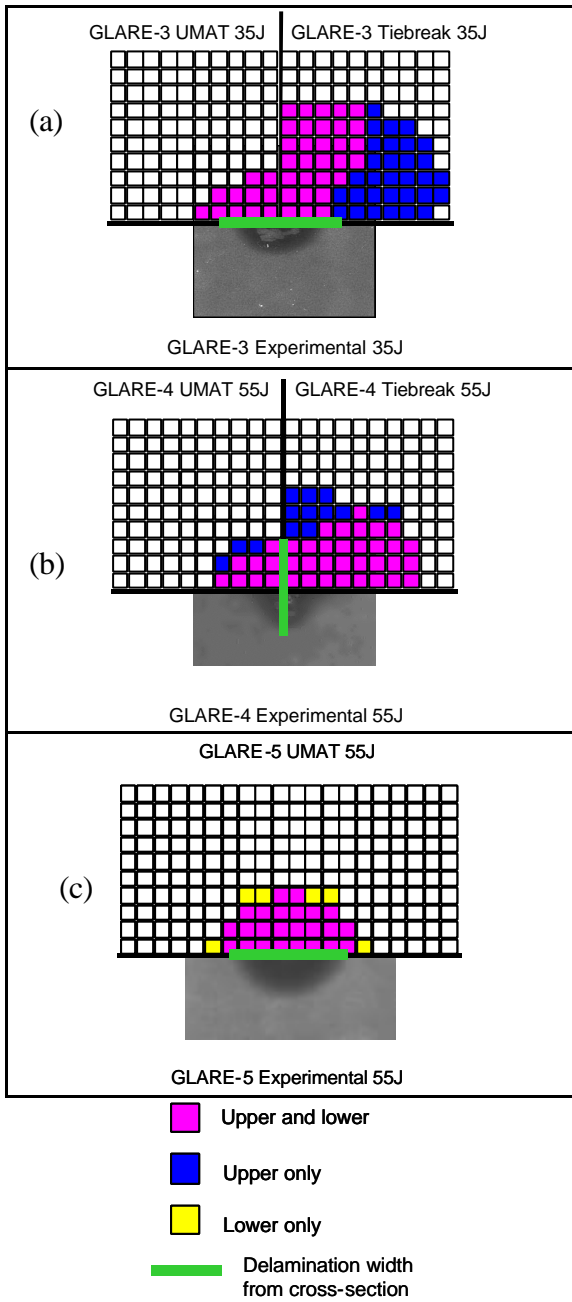
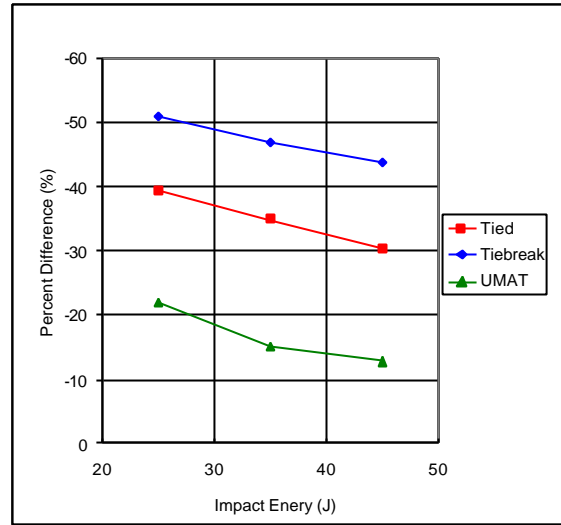Fig. 7. Sample damage maps for (a) GLARE-3, (b) GLARE-4 and (c) GLARE-5 with comparisons to experimental data.

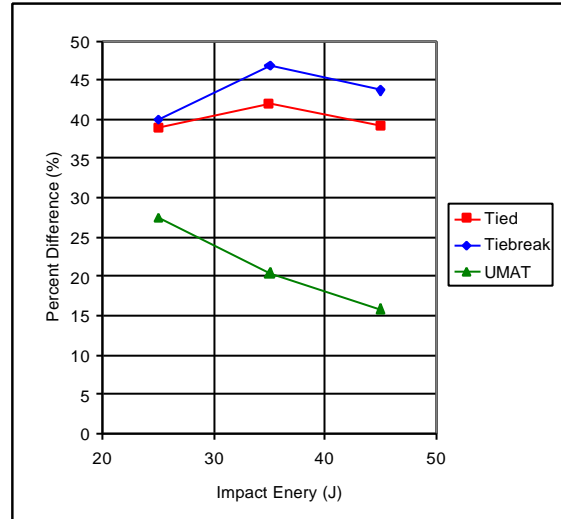Fig. 8. Difference between predicted and measured absorbed energy.

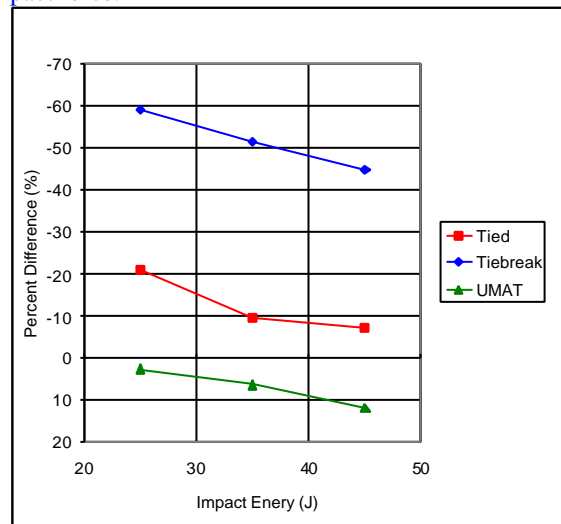Fig 9. Difference between predicted and measured peak impact force.

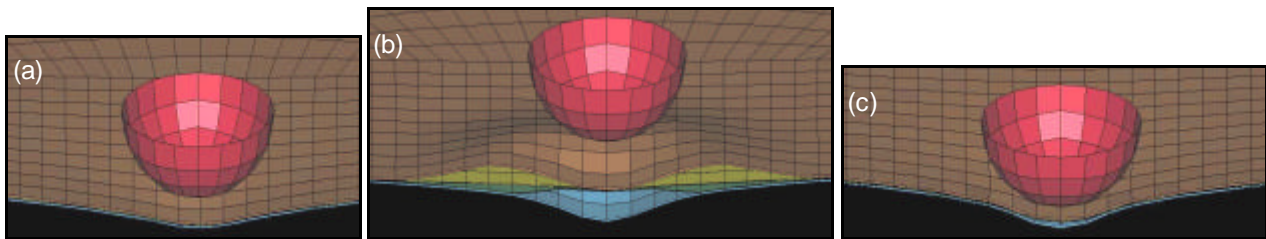Fig. 10. Difference between predicted and measured permanent dent depth.

Fig. 11. Sample impacted panel geometry for GLARE-3-2/1 impacted at 45 J with (a) tied-interface, (b) tiebreak-interface and (c) tiebreak-interface with UMAT material model.

The UMAT simulation, using the tiebreak interface under-predicted the absorbed energy. However, the results were a substantial improvement over the previous simulations. As well, the permanent dent depth was over-predicted by a smaller percentage than the previous simulations. Finally, the peak impact force was over-predicted by a significantly lower amount than the simulations described above. Based on these results, it is postulated that the formation of intralaminar damage has a greater effect on the impact response of FMLs than the formation of delamination damage. One can imagine that the combined surface area of the multitude of matrix cracks formed in the prepreg layers is much larger than the area formed by the delamination. Therefore, the energy released by formation of the matrix cracks would be proportionally larger than that released by the formation of delamination.

Interestingly, the inclusion of damage in prepreg layers resulted in an over prediction rather than an under-prediction of the permanent dent depth. The reasons for this are not readily discernible.

5 Conclusions

A user-defined material subroutine using a continuum damage mechanics based material model was successfully developed and used to predict the impact response GLARE panels.

The UMAT, with the tiebreak-interface delamination model, showed some sensitivity to the mesh density. Lower mesh densities resulted in an over-prediction of the extent of the delamination damage and an under-prediction of the dent depth.

As discussed, delamination does not appear to be the most important damage mode in impacted GLARE laminates. Cracking and strength deterioration in the prepreg layers is more influential and is responsible for the majority of the energy absorbed in low-velocity impacts. However, delamination damage needs to be considered when examining the post-impact mechanical properties of GLARE laminates.

The geometry of delamination damage in the impacted panels was accurately predicted using the CDM-based damage model. The geometry and the size of the predicted delaminated regions agreed with the experiments. As was observed in the experiments, the predicted damage was affected by the lay-up of the coupons.

References

[1] Kaufman, JG. Fracture Toughness of 7075-T6 and –T651 Sheet, Plate and Multi-Layered Adhesive-Bonded Panels. *Journal of Basic Engineering*, Vol. 89, pp 503-507, 1967.

[2] Vlot, A and Gunnink, JW. *Fibre Metal Laminates – An Introduction*, Kluwer Academic, 2002.

[3] Asundi, A and Choi, YN. Fiber Metal Laminates: An Advanced Material for Future Aircraft. *Journal of Materials Processing Technology*, Vol. 63, pp. 386-394, 1997.

[4] Gregory, MA and Roebroeks, GHJJ. Fibre-metal-laminates: A Solution to Weight, Strength and Fatigue Problems. *30th Annual CIM Conference of Metallurgists.* Ottawa, Canada, pp. 43-56, 1991.

[5] Laliberté, J, Poon, C and Straznicky, PV. *Durability Testing of Fibre-Metal-Laminates*, IAR Report LTR-ST-2231, NRCC, 1999.

[6] Laliberté, J, Poon, C and Straznicky, PV. Low-Velocity Impact Damage in GLARE Fibre-Metal Laminates. *12th International Conference on Composite Materials (ICCM)*, Paris, France, 1999.

[7] Laliberté, J, Poon, C and Straznicky, PV. Impact Damage Tolerance in Composites and Fibre Metal Laminates. *Canada-Taiwan Symposium on Aircraft Materials Testing, Maintenance and Repair*, Ottawa, Canada, 1999.

[8] Laliberté, J, Poon, C, Straznicky, PV and Fahr, A. Post-Impact Fatigue in Fiber-Metal Laminates. *2nd International Conference on the Fatigue of Composites (ICFC-2)*, Williamsburg, USA, 2000.

[9] Laliberté, J, Poon, C Straznicky, PV, Fawaz. Z and McCuaig, K. Post-Impact Biaxial Fatigue Crack Growth in GLARE. *21st ICAF Symposium,* Toulouse, France, 2001.

[10] Laliberté, J, Straznicky, PV and Poon, C. Post Impact Shear Behaviour in GLARE. *3rd Canadian International Composites Conference.* Montreal, Canada, 2001.

[11] Vlot, A. *Low-Velocity Impact Loading on Fibre Reinforced Aluminum Laminates (ARALL and GLARE) and other aircraft sheet materials,* TUDelft Report Number LR-718, 1993.

[12] Vlot, A, Kroone, E and Larocca, I. Impact Response of Fibre-metal-laminates. *Key Material Technologies*, Vol. 141-143, pp. 235-276, 1998.

[13] Majeed, O, Worswick, MJ, Straznicky, PV and Poon, C. Numerical Modelling of Transverse Impact on Composite Coupons. *CASI Journal.* Vol. 40, pp. 99-107, 1994.

[14] Wu, HF and Sun, CT. Impact Damage Characterization of Aramid Aluminum Laminates. *ICCM-9*, Spain, 1993.

[15] NASA Reference Publication 1092. *Standard Tests for Toughened Resin Composites*, NASA, 1983.

[16] Johnson, WS. *Impact and Residual Fatigue Behaviour of ARALL and AS6/5245 Composite Materials.* NASA Technical Memorandum 89013, NASA Langley Research Center, 1986.

[17] Hoogsteden, WP. *Compression After Impact Behaviour of ARALL®-1 Laminates.* Wright Laboratory, Wright-Patterson AFB, 1992.

[18] Poston, K. *Impact Properties and Related Applications of Fibre-metal-laminates.* Structural Laminates Corporation TD-M-94-007, 1994.

[19] Liaw, BM, Liu, YX and Villars, EA. Impact Damage Mechanisms in Fiber-Metal Laminates. *SEM Annual Conference*, Portland, USA, 2001.

[20] Hurez, A, Roelandt, JM and Abisor, A. Numerical Modelling of Elastic-Plastic Behaviour Coupled with Damage in Metal/Composite Laminates. Application to ARALL and GLARE. *ICCM-9*, Spain, 1993.

[21] Hashagen, F, Schellekens, JCJ, Borst, R de and Parisch, H. Finite Element Procedure for Modelling Fibre Metal Laminates. *Composite Structures*, Vol. 32, No. 1, pp. 255-264, 1995.

[22] Hashagen, F, de Borst, R and de Vries, T. Delamination Behavior of Spliced Fiber Metal Laminates Part 2. Numerical Investigation. *Composite Structures*, Vol. 46, pp.147-162, 1999.

[23] Hallquist, J. *LS-DYNA Theoretical Manual*, Livermore Software Technology Corporation, 1998.

[24] Hoof, J van, "Modeling of Impact Induced Delamination in Composite Materials," PhD Thesis, Ottawa-Carleton Institute for Mechanical and Aerospace Engineering, 1999.

[25] Laliberté, J, Straznicky, PV and Poon, C. Mode-I Delamination in Cross-Ply Fibre-Metal Laminates. *10th International Congress of Fracture (ICF-10).* Honolulu, USA, 2001.

[26] Kachanov, LM. On Creep Rupture Time. *Izv. Acad. Nauk SSSR, Otd. Techn. Nauk*. No. 8, pp. 26-31, 1958 [in Russian].

[27] Chaboche, JL. Continuum Damage Mechanics: Part 1 – General Concepts. *Journal of Applied Mechanics*, Vol. 55, pp. 59-64, 1988.

[28] Lemaitre, J. A Course on Damage Mechanics. Springer-Verlag, 1992.

[29] Ladevèze, P and Le Dantec, E. Damage Modelling of the Elementary Ply for Laminated Composites. *Composites Science and Technology.* Vol. 43, pp. 257-267, 1991.

[30] Hurez, A, Roelandt, JM and Abisor, A. Numerical Modelling of Elastic-Plastic Behaviour Coupled with Damage in Metal/Composite Laminates. Application to ARALL and GLARE. *ICCM-9*, Madrid, Spain, 1993.